# Young's Modulus and Its Orientation Dependence in β-$Ga_2O_3$ Thin Films Resolved by Nanomechanical Resonators

Xu-Qian Zheng[1], Hongping Zhao[2], Xutang Tao[3], and Philip X.-L. Feng[1*]

[1]*Department of Electrical and Computer Engineering, Herbert Wertheim College of Engineering, University of Florida, Gainesville, FL 32611, USA*
[2]*Department of Electrical and Computer Engineering, Ohio State University, Columbus, OH 43210, USA*
[3]*State Key Laboratory of Crystal Materials and Key Laboratory of Functional Crystal Materials and Device, Shandong University, Jinan, Shandong 250100, China*

**We report on the non-destructive measurement of Young's modulus of single crystal beta gallium oxide (β-$Ga_2O_3$) out of its nanoscale mechanical structures by measuring their fundamental mode resonance frequencies. From the measurements, we extract a Young's modulus in (100) plane, $E_{Y,(100)}$ = 261.4 GPa, for β-$Ga_2O_3$ nanoflakes synthesized by low-pressure chemical vapor deposition (LPCVD), and a Young's modulus in [010] direction, $E_{Y,[010]}$ = 245.8 GPa, for β-$Ga_2O_3$ nanobelts mechanically cleaved from bulk β-$Ga_2O_3$ crystal grown by edge-defined film-fed growth (EFG) method. The Young's moduli extracted directly on nanomechanical resonant device platforms are comparable to theoretical values from first-principle calculations and experimentally extracted values from bulk crystal. This study yields important quantitative nanomechanical properties of β-$Ga_2O_3$ crystals, and helps pave the way for further engineering of β-$Ga_2O_3$ M/NEMS transducers.**

***Keywords***: *β-gallium oxide (β-$Ga_2O_3$), Young's modulus, suspended nanostructure, nanomechanics, resonance, micro/nanoelectromechanical systems (M/NEMS)*

[*]Corresponding Author. Email: philip.feng@ufl.edu

# I. Introduction

Beta phase gallium oxide (β-$Ga_2O_3$) is the most stable polymorph of gallium oxide at ambient conditions. In addition, the monoclinic crystal structure of β-$Ga_2O_3$ is the only crystal structure that can be grown from the melt, contributing to strong potential in cost-effective mass production of high quality, high volume β-$Ga_2O_3$ single crystal for wafer scale device fabrication. Intriguingly, β-$Ga_2O_3$, as a semiconductor with an ultra-wide bandgap (UWBG, $E_g \approx 4.8$eV), [1,2] also possesses outstanding properties in electronic, photonic and mechanical domains. Thanks to its UWBG, β-$Ga_2O_3$ can hold very high electrical field before breaking down (up to $E_{br}$ = 8 MV/cm theoretically).[3,4] The high breakdown field enables the material for power and radio frequency (RF) electronic applications.[3,4,5] The bandgap at $E_g$ = 4.8 eV also introduce a photon absorption edge at the cutting off wavelength of solar-blind ultraviolet (SBUV) light, making the material attractive for artificial light detection in UV regime.[6,7] Further, β-$Ga_2O_3$ has excellent Young's modulus ($E_Y$ = 230–280 GPa),[8,9,10,11,12] favorable for micro/nanoelectromechanical systems (M/NEMS) applications. On one hand, β-$Ga_2O_3$ M/NEMS can supplement the rapidly emerging β-$Ga_2O_3$ power and RF electronics.[13,14] On the other hand, the β-$Ga_2O_3$ M/NEMS transducers are complimentary to β-$Ga_2O_3$ optoelectronics for SBUV detection.[15,16] However, the development of β-$Ga_2O_3$ M/NEMS is still burdened by the limited understanding in mechanical properties of β-$Ga_2O_3$ crystal. The Young's modulus of β-$Ga_2O_3$ crystal has only been studied in a handful of investigations experimentally or theoretically.[8,9,10,11,12] Determination of Young's modulus of β-$Ga_2O_3$ in micro- and nano-scale structures along with its dependency to the anisotropic crystal structure is desired for accelerating the development of β-$Ga_2O_3$ M/NEMS.

In this paper, we demonstrate non-destructive Young's modulus extraction for β-$Ga_2O_3$ crystal by measuring resonance frequencies from two different types of β-$Ga_2O_3$ nanomechanical

structures produced by different growth methods. The first type of device takes the form of nanodisks clamped at circular perimeter. The devices are fabricated using β-$Ga_2O_3$ nanoflakes grown by low-pressure chemical vapor deposition (LPCVD). The second type of device uses a doubly-clamped beam structure. The beam is constructed by mechanically cleaved β-$Ga_2O_3$ nanobelts from bulk crystal synthesized by edge-defined film-fed growth (EFG) method. The devices are carefully selected to ensure the dominance of flexural rigidity on the resonance frequency. We use ultrasensitive optical interferometry techniques to measure the resonance frequencies of the micro-/nano-mechanical structures.[11] Young's moduli from eight devices are extracted and compared to the values from the literature.

## II. Anisotropic Crystal Structure of β-$Ga_2O_3$

Figure 1 illustrates the crystal structure of β-$Ga_2O_3$ which belongs to monoclinic crystal system, with C2/m space group. Axes ***a***, ***b***, and ***c*** defines the unit cell of β-$Ga_2O_3$ crystal. Axes ***a*** and ***b*** are perpendicular to each other, while axis ***c*** has a $\beta = 103.7°$ angle to axis ***a***. The unit cell of β-$Ga_2O_3$ is anisotropic, where $a = 12.2$ Å, $b = 5.8$ Å, and $c = 3.0$ Å. To simplify the representation of directions in the crystal, we define an orthogonal coordinate system with respect to the unit cell of β-$Ga_2O_3$. The $x$ and $y$ axes coincide with $a$ ([100] direction) and $b$ ([010] direction) axes of β-$Ga_2O_3$ crystal, respectively. Therefore, we have $z$ axis perpendicular to $x$ and $y$ axes, which is 13.7° off from $c$ axis as shown in Fig. 1.

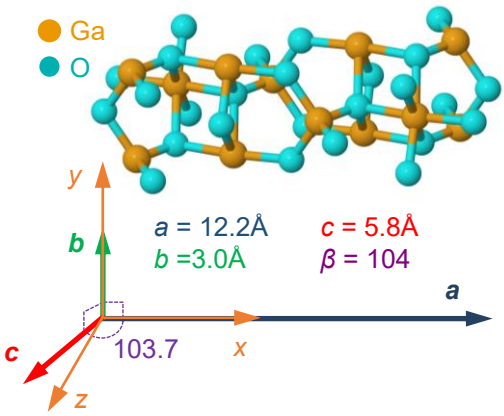


**Figure 1.** Schematic of monoclinic structure of β-$Ga_2O_3$ crystal with coordinative illustration of the relations between *x*, *y*, *z* directions and crystal orientations of β-$Ga_2O_3$.

## III. Young's Modulus of β-$Ga_2O_3$ Disks Grown by LPCVD

The first series (Series A) of β-$Ga_2O_3$ resonators are fabricated using β-$Ga_2O_3$ nanoflakes synthesized by low-pressure chemical vapor deposition (LPCVD) method on a 3C-SiC-on-Si substrate.[17] The devices in Series A are selected from the devices used in Ref. 11. Using high purity Ga pellets and $O_2$ (Ar as carrier gas) as source materials, β-$Ga_2O_3$ is grown on a 3C-SiC epi-layer on Si substrate at a growth temperature of 950 °C for 1.5 hours. The as-grown β-$Ga_2O_3$ is in the form of nanoflakes. We use thermal release tape to pick up the β-$Ga_2O_3$ nanoflakes and apply the nanoflakes to a 290nm-$SiO_2$-on-Si substrate with predefined microtrenches. Then, the structure is heated up to 90 °C. By gently removing the thermal release tape, the β-$Ga_2O_3$ nanoflakes are deposited on the substrate. The deposited β-$Ga_2O_3$ nanoflakes along with the pre-defined circular microtrenches form suspended nanostructures in the form of nanodisks clamped at the peripheral of the circular microtrenches.

We conduct electron backscatter diffraction (EBSD) measurement on multiple deposited β-$Ga_2O_3$ nanoflakes (Fig. 2a). The EBSD pole figures (Fig. 2b) suggest that the major surfaces of

the β-$Ga_2O_3$ nanoflakes are in parallel with the (100) plane of the crystal (perpendicular to the *x* direction in Fig. 1), while *y* (or [010]) and *z* directions are in parallel with the substrate plane.

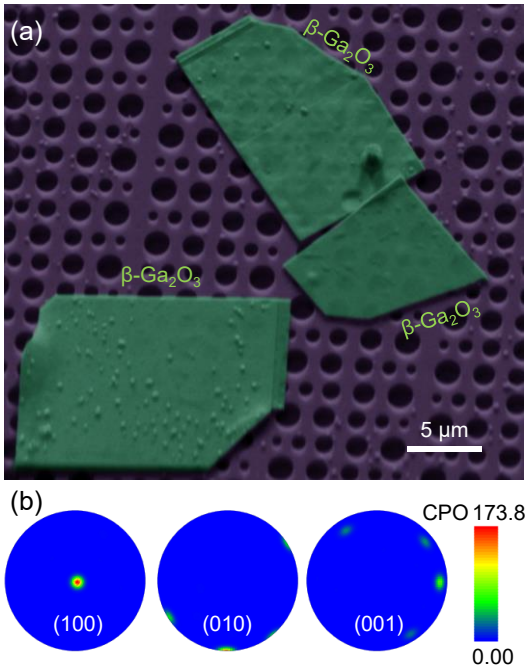


**Figure 2.** EBSD results of β-$Ga_2O_3$ flakes. (a) An SEM image of β-$Ga_2O_3$ nanoflakes on substrate with circular microtrenches. (b) EBSD pole figure for (100), (010), and (001) planes of the β-$Ga_2O_3$ flakes in (a). CPO: crystallographic preferred orientation.

Figure 3a shows a typical β-$Ga_2O_3$ disk (Device A1) suspended over a circular microtrench with a diameter of $d$ = 5.24 μm. EBSD measurement suggests that the β-$Ga_2O_3$ flake has its *x* axis pointing into the substrate (Fig. 3b), while the *y* and *z* directions are along the edges of the β-$Ga_2O_3$ flake. Using atomic force microscopy (AFM), we determine the thickness of the device as $h$ =61 nm (Fig. 3c). By measuring the thermomechanical noise resonance frequency of Device A1, we resolve a fundamental mode resonance at a frequency of $f_0$ = 39.6 MHz with a quality ($Q$) factor of $Q$ = 626. When the resonance frequency of such disk device is dominated by the flexural rigidity

of the suspended structure, *i.e.*, the device is in the 'disk' regime, the averaged Young's modulus in device plane can be revealed from measured fundamental-mode resonance frequency $f_0$ by[11,18]

$$E_{\mathrm{Y}} = \frac{3\pi^2 \rho\left(1-\nu^2\right) d^4}{\left(k_{\mathrm{A}0} r\right)^4 h^2} f_0^{\,2}, \tag{1}$$

where $\rho$ = 5950 kg/m$^3$ is the mass density of β-$Ga_2O_3$, $\nu$ = 0.2 is Poisson's ratio, and $k_{A0}r$ = 3.196 is the eigenvalue for the fundamental mode of a disk resonator clamped at the circular perimeter. Using Eq. (1) and the measured fundamental mode resonance frequency of Device A1, we extract a Young's modulus, $E_Y \approx 292$ GPa.

To further validate the extracted Young's modulus, we measure more β-$Ga_2O_3$ disk resonators. Figures 3e & 3f shows thermomechanical noise spectra of two β-$Ga_2O_3$ disk resonators, Device A2 and Device A3, respectively. We measure altogether five β-$Ga_2O_3$ disk resonators with thickness in 39 to 73 nm range, diameters among 3.20–5.24 μm, and fundamental mode resonance frequencies ranging from 39.6 MHz to 74.9 MHz. Thus, we extract an averaged Young's modulus of $E_{Y,(100)}$ = 261.4 GPa in (100) plane of β-$Ga_2O_3$ disk grown by LPCVD method. Table I summarizes the sizes, resonance frequencies and extracted Young's modulus of all Series A devices. Since fundamental mode resonance frequency of β-$Ga_2O_3$ disk scales linearly with the aspect ratio $h/d^2$ of the disk, we can plot the scaling using $E_Y$ = 261.4 GPa (Fig. 3g). All the measured data points are close to the scaling curve, indicating great precision in extracted Young's modulus.

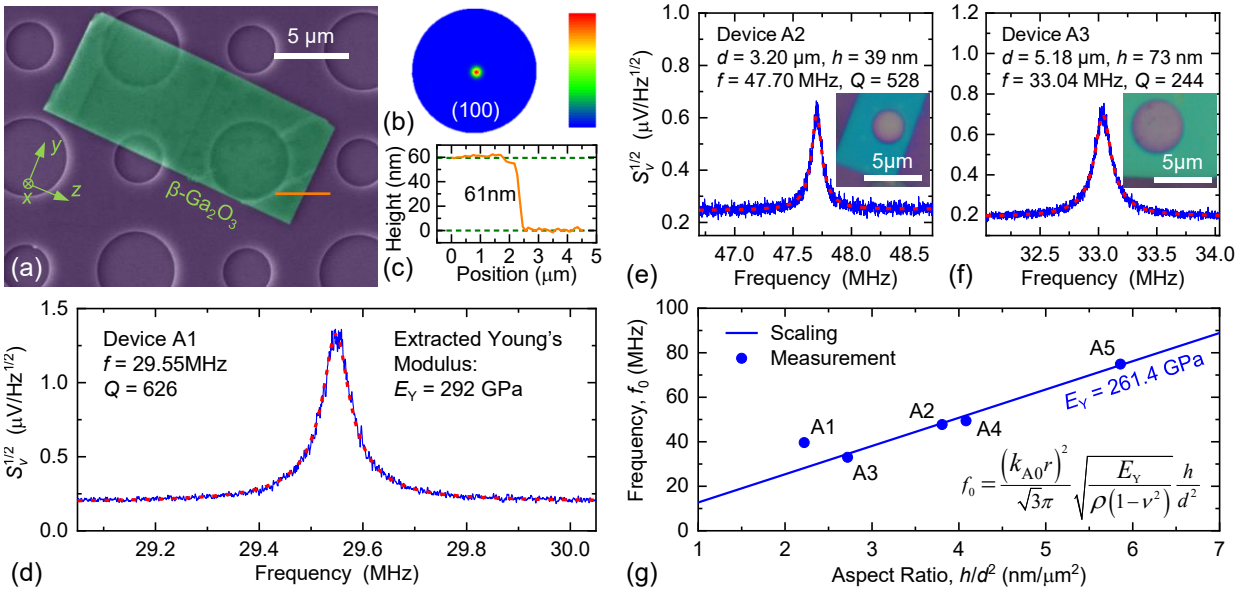


**Figure 3.** Young's modulus extraction from β-$Ga_2O_3$ disk resonators. (a) An SEM image of β-$Ga_2O_3$ disk resonator (Device A1). Coordinate labels indicate *x*, *y*, and *z* directions acquired from EBSD measurement. (b) EBSD pole figure for (100) plane of Device A1. (c) AFM trace corresponding to the orange line in (a). (d) Fundamental mode resonance spectrum of Device A1. (e) & (f) Fundamental mode resonance spectra of Devices A2 and A3, respectively. *Insets*: device images. (g) Frequency scaling with respect to aspect ratio $h/d^2$ using the extracted Young's modulus ($E_Y$ = 261.4 GPa) for LPCVD β-$Ga_2O_3$ crystal.

TABLE I. Extracted Young's Moduli from β-$Ga_2O_3$ Disk Resonators

| Device Number | Diameter $d$ (μm) | Thickness $h$ (nm) | Resonance Frequency $f_0$ (MHz) | Young's Modulus $E_Y$ (GPa) |
|---|---|---|---|---|
| A1 | 5.24 | 61 | 39.6 | 292 |
| A2 | 3.20 | 39 | 47.7 | 259 |
| A3 | 5.18 | 73 | 33.0 | 244 |
| A4 | 3.20 | 60 | 74.9 | 270 |
| A5 | 3.32 | 45 | 49.4 | 242 |
| Average | | | | 261.4 |

## IV. Young's Modulus of β-$Ga_2O_3$ Doubly-Clamped Beams Synthesized by EFG

We use the β-$Ga_2O_3$ nanobelts that are mechanically cleaved from bulk β-$Ga_2O_3$ crystal grown by edge-defined film-fed growth (EFG) method for fabrication of second series (Series B) of β-$Ga_2O_3$ devices.[19] During the fabrication, we first introduce bulk β-$Ga_2O_3$ crystal onto a piece of tape. After exfoliating the β-$Ga_2O_3$ for multiple iterations using the tape similar to exfoliation of two-dimensional (2D) materials, [20] we apply the exfoliated β-$Ga_2O_3$ flakes onto a polydimethylsiloxane (PDMS) stamp for transfer. Through observation under optical microscope, the exfoliated β-$Ga_2O_3$ flakes are in the form of nanobelts. Based on the bonding strength of different planes of monoclinic β-$Ga_2O_3$ crystal, the large surface of the β-$Ga_2O_3$ nanobelt is in parallel with the (100) plane of β-$Ga_2O_3$ crystal and the [010] direction (*y* axis) is going along with the long sides of the nanobelt. After identifying the β-$Ga_2O_3$ nanobelt with desired size and thickness, we transfer the nanobelt on PDMS to a 290 nm-SiO2-on-Si substrate with pre-defined rectangular microtrenches using the dry transfer technique.[20] The β-$Ga_2O_3$ nanobelt suspended over the microtrench forms a doubly-clamped beam structure. Figure 4a shows a typical β-$Ga_2O_3$ doubly-clamped beam resonator (Device B1). The device is 460 nm thick, suspended over a 20.6 μm long microtrench. The *x*, *y*, and *z* directions of β-$Ga_2O_3$ crystal are labeled in Fig. 4a based on the orientation of the β-$Ga_2O_3$ nanobelt. We fabricate and measure three β-$Ga_2O_3$ doubly-clamped beams. Device images of Devices B2 and B3 are shown in Figs. 4c & 4e, respectively. Figures 4b, 4d & 4f show the photothermally driven resonance spectrum of the fundamental mode resonance of Devices B1, B2, and B3, respectively. Similar to the β-$Ga_2O_3$ disk resonators, Young's modulus of the doubly-clamped beam can be extracted from measured resonance frequency when the resonance motion of the device is dominated by the flexural rigidity of the structure. Therefore, we have[21]

$$E_{\mathrm{Y}} = \frac{48\pi^2 \rho L^4}{\left(k_{\mathrm{B0}} L\right)^4 h^2} f_0^{\,2}, \tag{2}$$

where $L$ is the length of the doubly-clamped beam and $k_{\mathrm{B0}}L$ = 4.73 is the eigenvalue for the fundamental mode of a doubly-clamped beam. In this case, we can extract Young's modulus along the [010] direction ($y$ axis) of β-$Ga_2O_3$ crystal. Table II summarizes the sizes, resonance frequencies and extracted Young's modulus of all Series B devices. We have an averaged Young's modulus of $E_{\mathrm{Y}}$ = 245.8 GPa along [010] direction ($y$ axis). Similar to β-$Ga_2O_3$ disk resonators, the fundamental mode resonance frequency of β-$Ga_2O_3$ doubly-clamped beams scales linearly with the aspect ratio $h/L^2$. Thus we can also confirm the precision of Young's modulus extraction with the scaling curve in Fig. 4g.

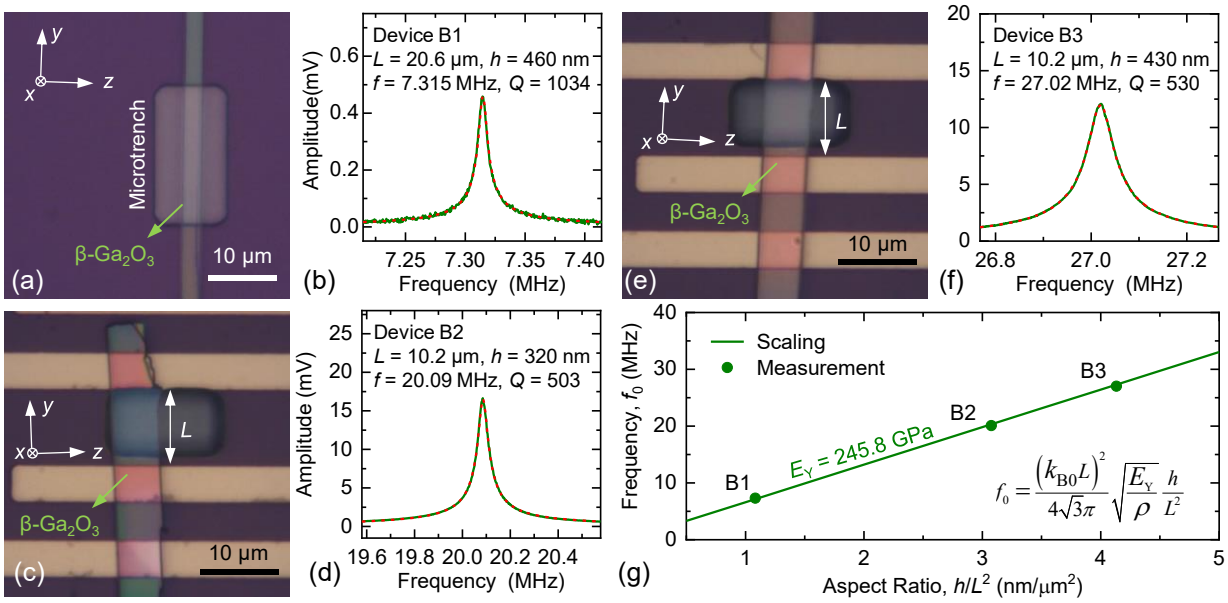


**Figure 4.** Young's modulus extraction from β-$Ga_2O_3$ doubly-clamped beam resonators. (a), (c) & (e) Optical image of β-$Ga_2O_3$ doubly-clamped beam resonators, Devices B1, B2, and B3, respectively. Coordinate labels indicate $x$, $y$, and $z$ directions based on the orientation of the β-$Ga_2O_3$ nanobelt. Lengths of Devices B2 and B3 are determined by the distances between the electrodes. (b), (d) & (f) Fundamental mode resonance spectra of Devices B1, B2, and B3, respectively. (g) Frequency scaling with respect to aspect ratio $h/L^2$ using the extracted Young's modulus ($E_{\mathrm{Y}}$ = 245.8 GPa) for EFG β-$Ga_2O_3$ crystal.

TABLE II. Extracted Young's Moduli from β-$Ga_2O_3$ Doubly-Clamped Beam Resonators

| Device Number | Length $L$ (μm) | Thickness $h$ (nm) | Resonance Frequency $f_0$ (MHz) | Young's Modulus $E_Y$ (GPa) |
|---|---|---|---|---|
| B1 | 20.6 | 460 | 7.315 | 256.4 |
| B2 | 10.2 | 320 | 20.09 | 240.3 |
| B3 | 10.2 | 430 | 27.02 | 240.7 |
| Average | | | | 245.8 |

## V. Discussions

Utilizing the measured fundamental mode resonance frequencies, we have extracted the Young's modulus in (100) plane for LPCVD grown β-$Ga_2O_3$ nanoflakes, and in [010] direction ($y$ axis) for exfoliated nanobelts from bulk crystal synthesized by EFG method. Though the monoclinic crystal structure of β-$Ga_2O_3$ gives rise to possibly anisotropic Young's modulus, our results and evidence from previous works suggest that the chance of strong in-plane Young's modulus anisotropy in (100) plane of β-$Ga_2O_3$ crystal, the suspended plane of both types of devices, is low. Multiple measured Young's modulus values of β-$Ga_2O_3$ in different directions, *e.g.*, $E_Y$ = 232 GPa for (100) plane of bulk β-$Ga_2O_3$,[10] $E_Y$ = 280GPa for nanowire,[8] and our $E_Y$ = 261.4 GPa for (100) plane and $E_Y$ = 245.8 for [010] direction ($y$ axis), are all close to each other, indicating that in certain directions the Young's modulus of β-$Ga_2O_3$ is similar. Using the theoretically calculated elasticity tensor matrix of β-$Ga_2O_3$ in Refs. 9 and 12, we can calculate the Young's modulus in $y$ and $z$ directions, $E_{Y,y}$ = 329 GPa, $E_{Y,z}$ = 298 GPa, and $E_{Y,y}$ = 263 GPa, $E_{Y,z}$ = 228 GPa, for Ref. 9 and Ref. 12, respectively. The derived results from elasticity tensor matrix indicate insignificant anisotropy of Young's modulus in the lateral directions ($y$ and $z$) of β-$Ga_2O_3$ flakes. Thus our

measured Young's modulus $E_Y$ = 261.4 GPa from LPCVD β-$Ga_2O_3$ nanoflakes is accurate as the average Young's modulus for (100) (*y*-*z*) plane of the β-$Ga_2O_3$.

## VI. Conclusions

In conclusion, we have demonstrated the extraction of Young's modulus in (100) plane, $E_{Y,(100)}$ = 261.4 GPa, for LPCVD grown β-$Ga_2O_3$ nanoflakes and Young's modulus in [010] direction, $E_{Y,[010]}$ = 245.8 GPa, of β-$Ga_2O_3$ nanobelts exfoliated from EFG synthesized bulk β-$Ga_2O_3$ crystal, using the measured fundamental mode resonance frequencies of β-$Ga_2O_3$ micro-/nano-mechanical structures. These extracted Young's moduli are comparable to those obtained from bulk crystal experimentally or from theoretical calculations, indicating no clear size effect on Young's modulus for β-$Ga_2O_3$ down to 10s of nm scale. This work provides essential information regarding mechanical properties in nanoscale β-$Ga_2O_3$ crystal for future design and development of β-$Ga_2O_3$ M/NEMS devices for power, RF and optical sensing applications.

**Data Availability Statement:** Data available in article.

**Acknowledgement:** We thank the financial support from the Defense Threat Reduction Agency (DTRA) Basic Scientific Research Program (Grant No. HDTRA1-19-1-0035).

**References**


[1] M. R. Lorenz, J. F. Woods, and R. J. Gambino, "Some Electrical Properties of the Semiconductor β-$Ga_2O_3$," J. Phys. Chem. Solids **28**, 403-404 (1967).

[2] N. Ueda, H. Hosono, R. Waseda, and H. Kawazoe, "Anisotropy of Electrical and Optical Properties in β-$Ga_2O_3$ Single Crystals," Appl. Phys. Lett. **71**, 933 (1997).

[3] M. Higashiwaki, K. Sasaki, A. Kuramata, *et al.*, "Gallium Oxide ($Ga_2O_3$) Metal-Semiconductor Field-Effect Transistors on Single-Crystal β-$Ga_2O_3$ (010) Substrates," Appl. Phys. Lett. **100**, 013504 (2012).

[4] M. Higashiwaki, K. Sasaki, H. Murakami, *et al.*, "Recent Progress in $Ga_2O_3$ Power Devices," Semicond. Sci. Technol. **31**, 034001 (2016).

[5] A. J. Green, K. D. Chabak, M. Baldini, *et al.*, "β-$Ga_2O_3$ MOSFETs for Radio Frequency Operation," IEEE Electron Device Lett. **38**, 790-793 (2017).

[6] W.-Y. Kong, G.-A. Wu, K.-Y. Wang, *et al.*, "Graphene-β-$Ga_2O_3$ Heterojunction for Highly Sensitive Deep UV Photodetector Application," Adv. Mater. **28**, 10725- 10731 (2016).

[7] R. Lin, W. Zheng, D. Zhang, *et al.*, "High-Performance Graphene/β-$Ga_2O_3$ Heterojunction Deep-Ultraviolet Photodetector with Hot-Electron Excited Carrier Multiplication," ACS Appl. Mater. Interfaces **10**, 22419-22426 (2018).

[8] M.-F. Yu, M. Z. Atashbar, and X. Chen, "Mechanical and Electrical Characterization of β-$Ga_2O_3$ Nanostructures for Sensing Applications," IEEE Sens. J. **5**, 20-25 (2005).

[9] W. Miller, K. Böttcher, Z. Galazka, and J. Schreuer, "Numerical modelling of the Czochralski growth of β-$Ga_2O_3$," Cryst. **7**, 26 (2017).

[10] V.I. Nikolaev, V. Maslov, S.I. Stepanov, *et al.*, "Growth and Characterization of β-$Ga_2O_3$ Crystals," J. Cryst. Growth **457**, 132-136 (2017).

[11] X.-Q. Zheng, J. Lee, S. Rafique, *et al.*, "Ultrawide Band Gap β-$Ga_2O_3$ Nanomechanical Resonators with Spatially Visualized Multimode Motion," ACS Appl. Mater. Interfaces **9**, 43090-43097 (2017).

[12] A. S. Grashchenko, S. A. Kukushkin, V. I. Nikolaev, *et al.*, "Study of the Anisotropic Elastoplastic Properties of β-$Ga_2O_3$ Films synthesized on SiC/Si Substrates," Phys Solid State **60**, 852-857 (2018).

[13] X.-Q. Zheng, J. Lee, and P. X.-L. Feng, "Beta Gallium Oxide (β-$Ga_2O_3$) Vibrating Channel Transistor," in Proc. IEEE 33rd Int. Conf. on Micro Electro Mechanical Systems (MEMS), Vancouver, BC, Canada, 18-22 Jan. 2020, pp. 186-189.

[14] X.-Q. Zheng, T. Kaisar, and P. X.-L. Feng, "Electromechanical Coupling and Motion Transduction in β-$Ga_2O_3$ Vibrating Channel Transistors," Appl. Phys. Lett. **117**, 243504 (2020).

[15] X.-Q. Zheng, J. Lee, S. Rafique, *et al.*, "β-$Ga_2O_3$ NEMS Oscillator for Real-Time Middle Ultraviolet (MUV) Light Detection," IEEE Electron Device Lett. **39**, 1230-1233 (2018).

[16] X.-Q. Zheng, Y. Xie, J. Lee, *et al.*, "Beta Gallium Oxide (β-$Ga_2O_3$) Nanoelectromechanical Transducer for Dual-Modality Solar-Blind Ultraviolet Light Detection," APL Mater. **7**, 022523 (2019).

[17] S. Rafique, L. Han, J. Lee, *et al.*, "Synthesis and Characterization of $Ga_2O_3$ Nanosheets on 3C-SiC-on-Si by Low Pressure Chemical Vapor Deposition," J. Vac. Sci. Technol. B **35**, 011208 (2017).

[18] H. Suzuki, N. Yamaguchi, and H. Izumi, "Theoretical and Experimental Studies on the Resonance Frequencies of a Stretched Circular Plate: Application to Japanese Drum Diaphragms," Acoust. Sci. Technol. **30**, 348-354 (2009).

[19] W. Mu, Z. Jia, Y. Yin, *et al.*, "One-Step Exfoliation of Ultra-Smooth β-$Ga_2O_3$ Wafers from Bulk Crystal for Photodetectors," CrystEngComm **19**, 5122-5127 (2017).

[20] R. Yang, X.-Q. Zheng, Z. Wang, *et al.*, "Multilayer $MoS_2$ Transistors Enabled by a Facile Dry-Transfer Technique and Thermal Annealing," J. Vac. Sci. Technol. B **32**, 061203 (2014).

[21] S. Timoshenko, D. H. Young, and W. Weaver, Vibration Problems in Engineering, Forth Edition (John Wiley & Sons, New York, 1974).